Supporting Information

Crystal facet dependence of ketonization of propionic acid on anatase TiO_2

Jiao Huang,‡[a] Liwen Li,‡[a] Xiaoxia Wu,[a] Yonghua Guo,[a] Zijun Yang,[a] Hua Wang,[a] Qingfeng Ge[b] and Xinli Zhu*[ac]

[a] *Collaborative Innovation Center of Chemical Science and Engineering, Key Laboratory for Green Chemical Technology of Ministry of Education, School of Chemical Engineering and Technology, Tianjin University, Tianjin, 300072, China*

[b] *Department of Chemistry and Biochemistry, Southern Illinois University, Carbondale, IL, 62901, United States*

[c] *Haihe Laboratory of Sustainable Chemical Transformations, Tianjin, 300192, China*

‡ These authors contributed equally.

* Corresponding Author.

Email address: xinlizhu@tju.edu.cn (X.L. Zhu)

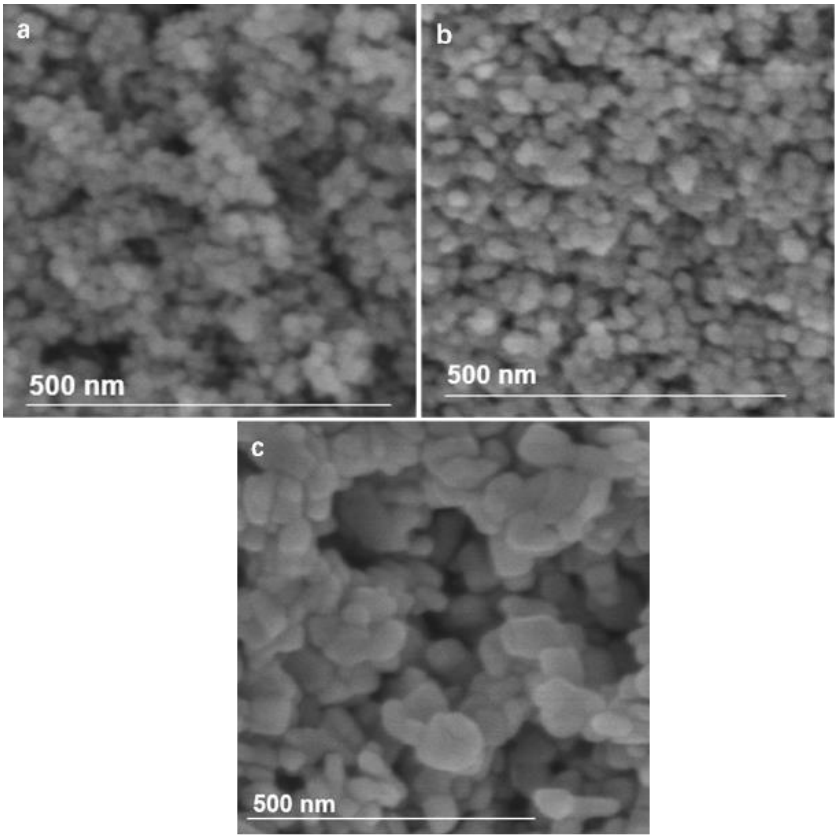

Fig. S1 SEM images for (a) TiO_2(101), (b) TiO_2(100) and (c) TiO_2(001).

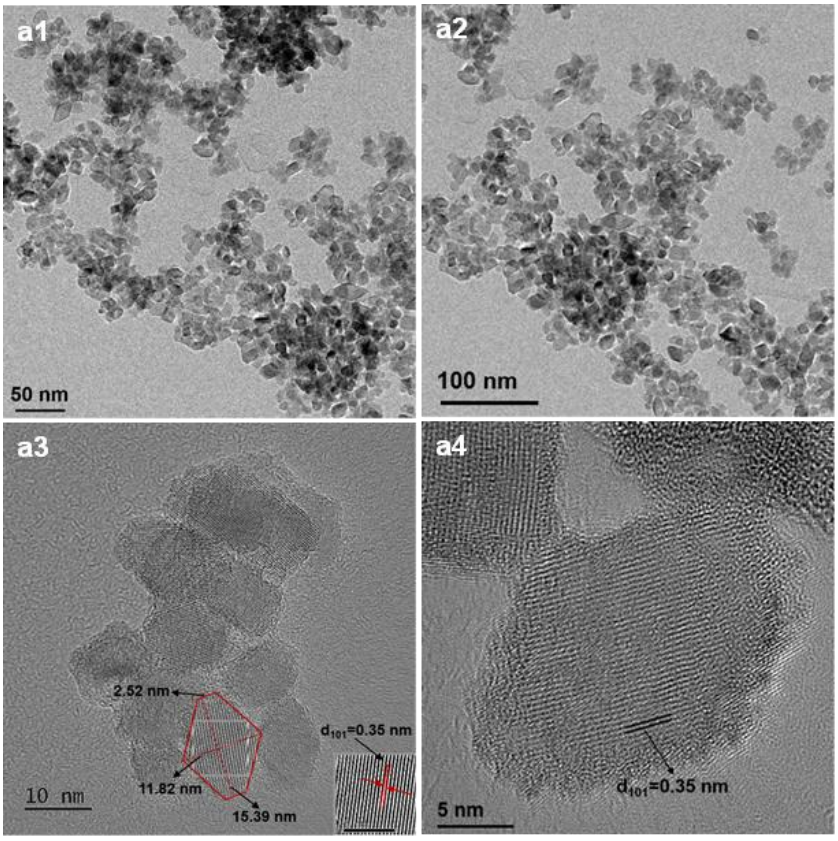

Fig. S2 TEM images for TiO_2(101).

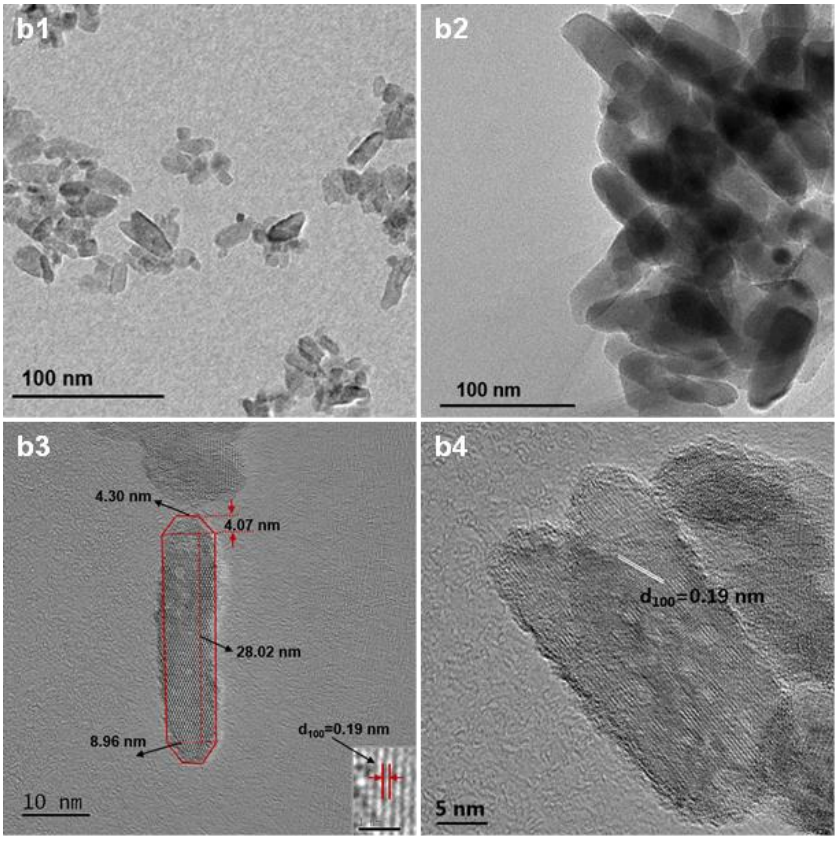

Fig. S3 TEM images for TiO_2(100).

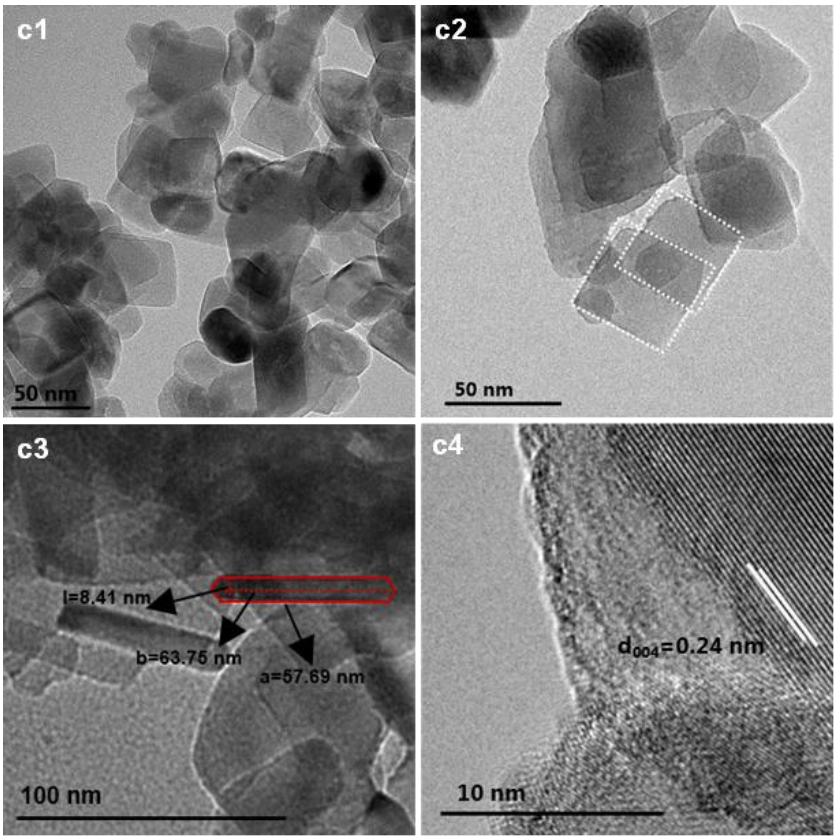

Fig. S4 TEM images for TiO_2(001).

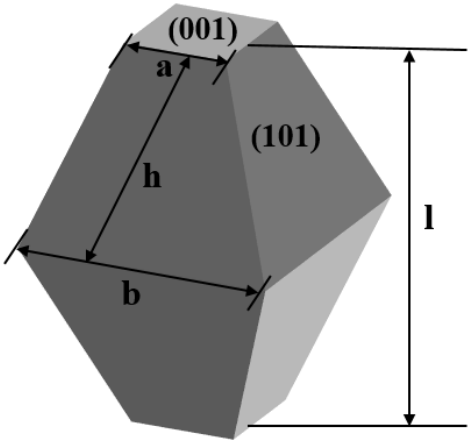

Fig. S5 Calculation of facets percentage of TiO_2(101).

$$a = 2.52\ nm$$
$$b = 11.82\ nm$$
$$l = 15.39\ nm$$

$$h^2 = (\frac{b-a}{2})^2 + (\frac{l}{2})^2$$
$$S_{001} = a^2$$
$$S_{101} = \frac{1}{2} \times (a+b) \times h$$
$$percentage\ of\ 101 = \frac{S_{101} \times 8}{S_{101} \times 8 + S_{001} \times 2} = 97.6\%$$
$$percentage\ of\ 001 = \frac{S_{001} \times 2}{S_{101} \times 8 + S_{001} \times 2} = 2.4\%$$

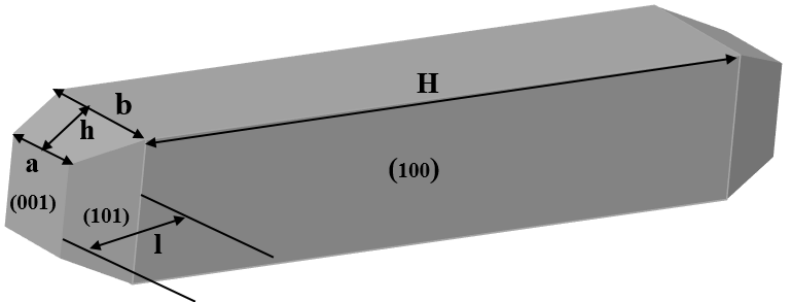

Fig. S6 Calculation of facets percentage of TiO_2(100).

$$a = 4.30\ nm$$
$$b = 8.96\ nm$$
$$l = 4.07\ nm$$
$$H = 28.02\ nm$$

$$h^2 = (\frac{b-a}{2})^2 + (l)^2$$
$$S_{001} = a^2$$
$$S_{100} = b \times H$$
$$S_{101} = \frac{1}{2} \times (a+b) \times h$$

$$percentage\ of\ 100 = \frac{S_{100} \times 4}{S_{101} \times 8 + S_{001} \times 2 + S_{100} \times 4} = 77.8\%$$

$$percentage\ of\ 101 = \frac{S_{101} \times 8}{S_{101} \times 8 + S_{001} \times 2 + S_{100} \times 4} = 19.3\%$$

$$percentage\ of\ 001 = \frac{S_{001} \times 2}{S_{101} \times 8 + S_{001} \times 2 + S_{100} \times 4} = 2.9\%$$

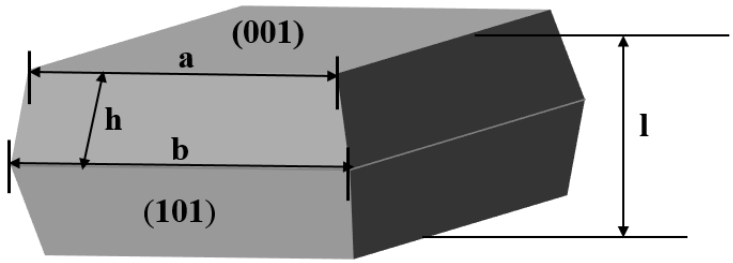

Fig. S7 Calculation of facets percentage of TiO_2(001).

$$a = 57.69\ nm$$

$$b = 63.75\ nm$$

$$l = 8.41\ nm$$

$$h^2 = (\frac{b-a}{2})^2 + (\frac{l}{2})^2$$

$$S_{001} = a^2$$

$$S_{101} = \frac{1}{2} \times (a+b) \times h$$

$$percentage\ of\ 001 = \frac{S_{001} \times 2}{S_{101} \times 8 + S_{001} \times 2} = 72.6\%$$

$$percentage\ of\ 101 = \frac{S_{101} \times 8}{S_{101} \times 8 + S_{001} \times 2} = 27.4\%$$

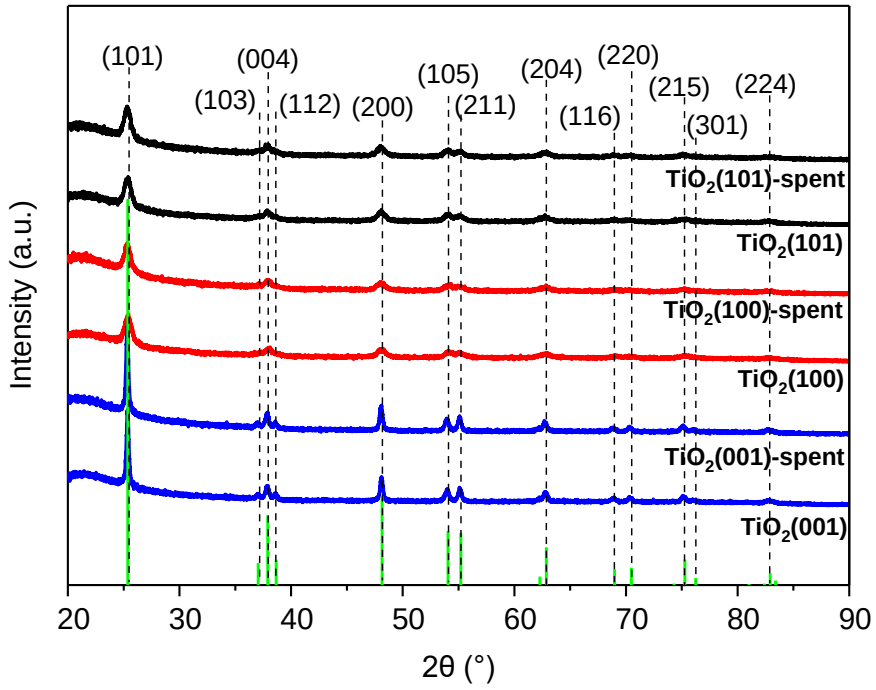

Fig. S8 X-ray diffraction patterns of spent TiO_2 catalysts. Reaction conditions: T = 350 °C, P_{total} =101.325 kPa, P_{acid} = 4.0 kPa, W/F = 0.2 h, reaction time = 10 h.

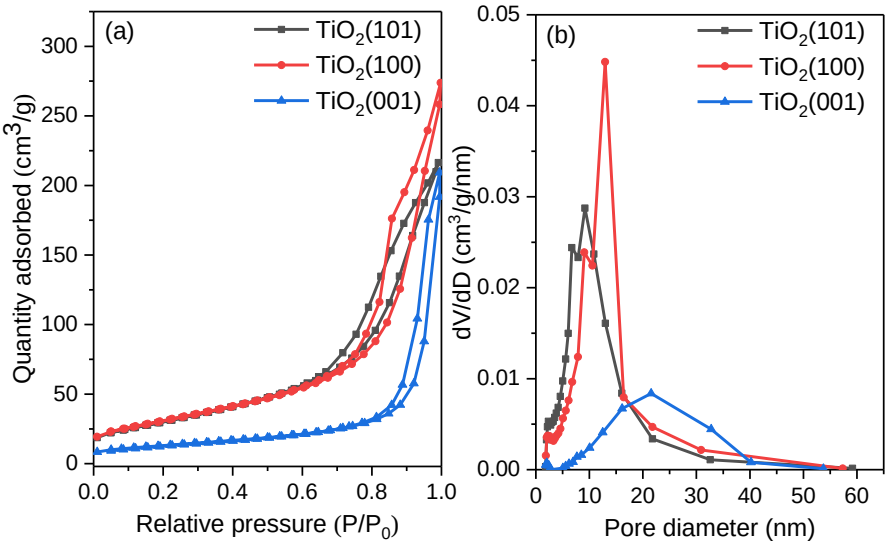

Fig. S9 N_2 adsorption and desorption isotherms (a) and BJH pore size distribution (b) on TiO_2 catalysts.

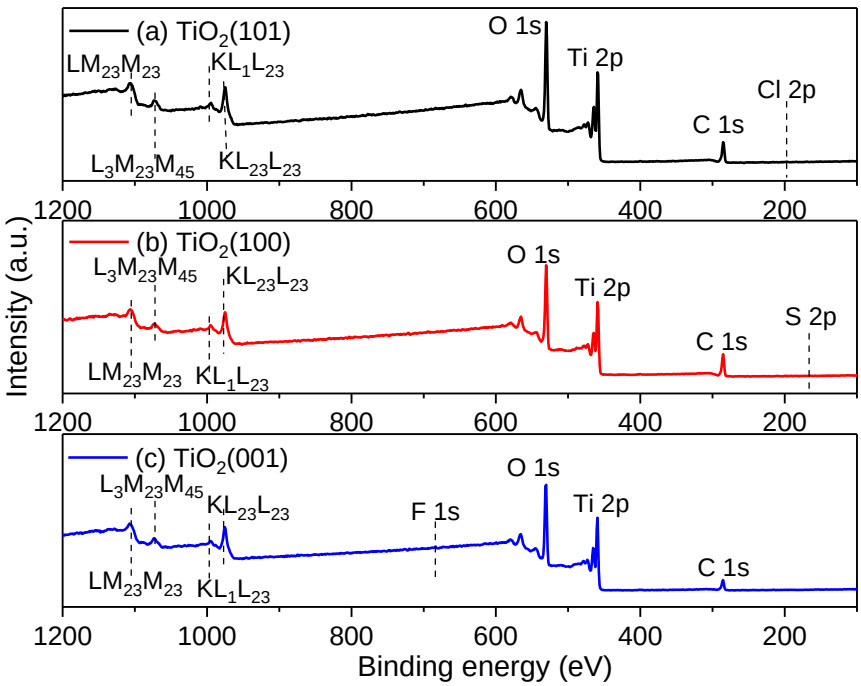

Fig. S10 XPS survey spectra of (a) TiO_2(101), (b) TiO_2(100) and (c) TiO_2(001).

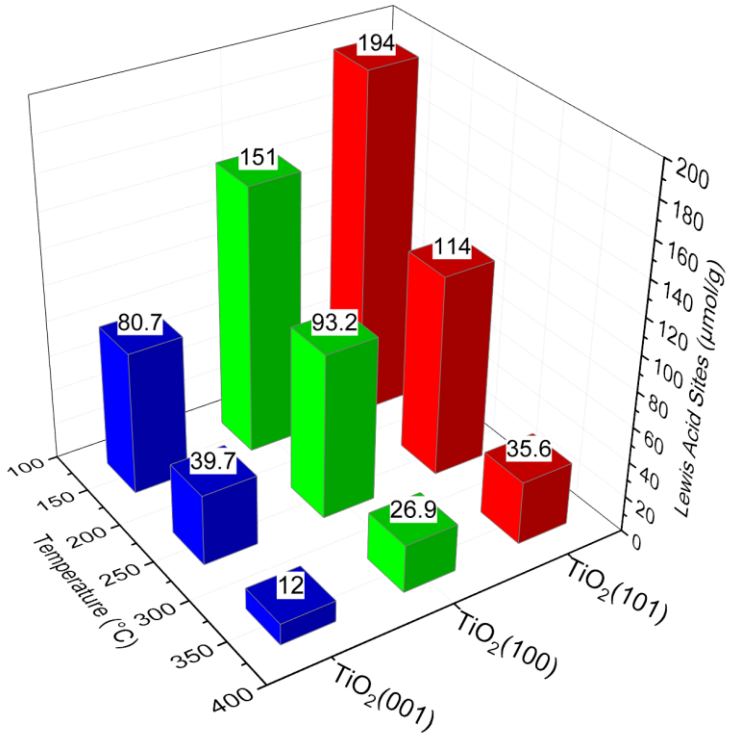

Fig. S11 The estimated Lewis acid sites densities determined by pyridine thermal desorption IR spectra on TiO_2 catalysts at 150 °C, 250 °C and 350 °C.

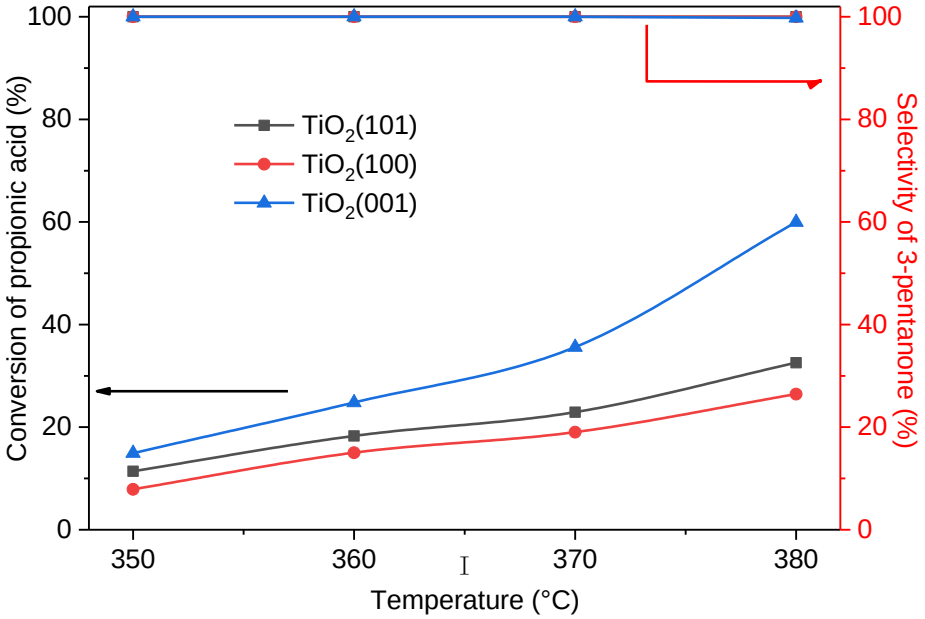

Fig. S12 Conversion of propionic acid and selectivity of 3-pentanone on the TiO_2 catalysts as a function of temperature. Reaction conditions: P_{total} = 101.325 kPa, P_{acid} = 4.0 kPa, W/F = 0.05 h.

Table S1 Comparison of ketonization of small carboxylic acid on different oxide catalysts.

Entry	Catalysts	Reaction condition	Conversion (%)	Selectivity (%)	Yield (%)	Reference
1	TiO_2(101)	a	11.39	100	11.39	this work
2	TiO_2(100)	a	7.87	100	7.87	this work
3	TiO_2(001)	a	14.92	100	14.92	this work
4	rutile	b	92	95	87.4	
5	brookite	b	56	95	53.2	[1]
6	anatase	b	10	77	7.7	
7	CeO_2	c	36.3	99.7	36.1	[2]
8	CeO_2−P	a	11.1	99.6	11.0	[3]
9	CeO_2−UiO-450	a	35.7	99.8	36.6	
10	CeO_2−R	a	65.6	>99	64.9	[4]
11	$Ce_{0.1}Zr_{0.9}O_2$	a	31.7	>95	30.4	[5]
12	t-ZrO_2	d	26	>97.5	25.4	[6]
13	Ca/Zn/AlO_x	e	92	100	92	[7]
14	Fe_3O_4/SiO_2	f	50	59	29.5	[8]
15	$0.17La_xZr_yO_z$	g	30	100	30	[9]
16	$CeFeO_x$	h	87	100	87	[10]
17	Zn-Cr (10:1)	i	70	100	70	[11]

a. Reaction conditions: T = 350 °C, P_{total} = 101.325 kPa, P_{acid} = 4.0 kPa, W/F = 0.05 h, and the reactant is propionic acid.

b. Reaction conditions: T = 375 °C, P_{total} = 101.325 kPa, WHSV = 3.24 h^{-1}, and the reactant is propionic acid.

c. Reaction conditions: T = 350 °C, P_{total} = 101.325 kPa, W/F = 0.08 h, propionic acid was fed into the reactor at the liquid flow rate of 6.5 $cm^3 \cdot h^{-1}$.

d. Reaction conditions: T = 350 °C, P_{total} = 101.325 kPa, P_{acid} = 4.0 kPa, W/F = 0.05 h, and the reactant is propionic acid.

e. Reaction conditions: T = 350 °C, 50 wt.% aqueous AcOH solution was pumped into the reactor with catalyst (100 mg) at a flow rate of 0.4 mL/h with N_2 as carrier gas (10 mL/min).

f. Reaction conditions: T = 410 °C, P_{total} = 101.325 kPa. N_2 was employed as the carrier gas (50 $mL \cdot min^{-1}$) and approximately 50 mg each of Fe_3O_4 and SiO_2 diluted with fused silica granules was used.

g. Reaction conditions: T = 295 °C, WHSV = 3.8 h^{-1}. All of the catalysts were tested at 9800 kPa with a feed composed of 10 wt. % acetic acid in H_2O.

h. Reaction condition: 0.3 g catalyst, 40 $mL \cdot min^{-1}$ N_2 flow rate, 0.03 $mL \cdot min^{-1}$ liquid flow rate, TOS = 1 h, W/F = 0.17 h.

i. Reaction condition: 1 bar pressure, 0.2 g catalyst, 20 $mL \cdot min^{-1}$ N_2 flow rate, 2 vol% propionic acid, 4 h time on stream, W/F = 4 $h \cdot g \cdot mol^{-1}$, T = 350 °C.

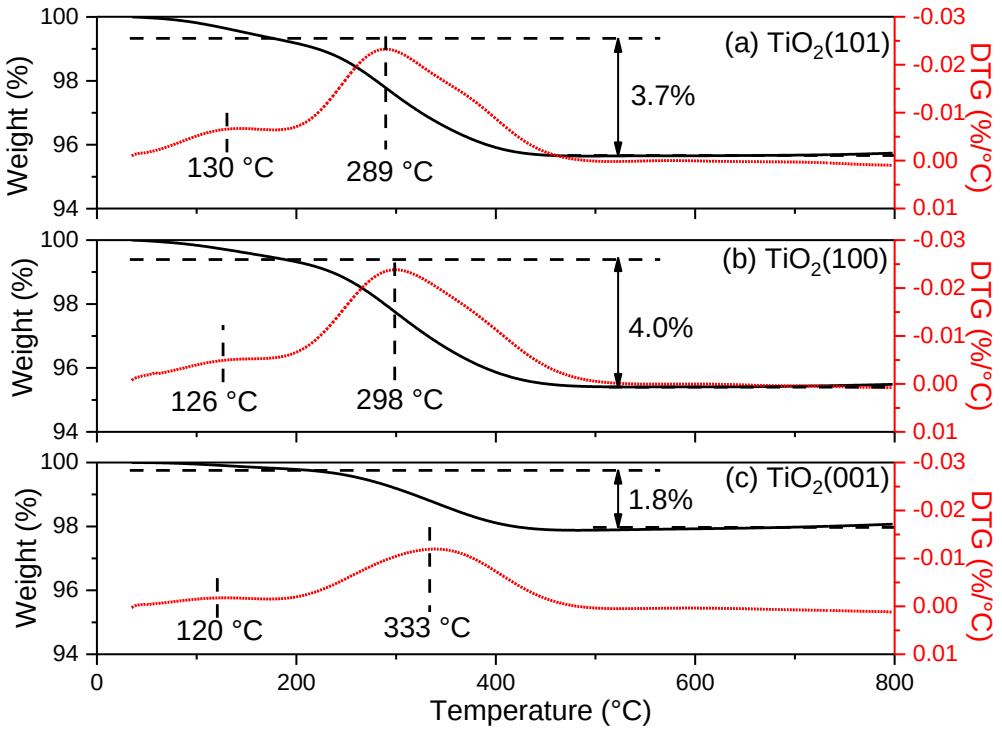

Fig. S13 Thermogravimetric and differential thermogravimetric curves for spent (a) TiO_2(101), (b) TiO_2(100) and (c) TiO_2(001).

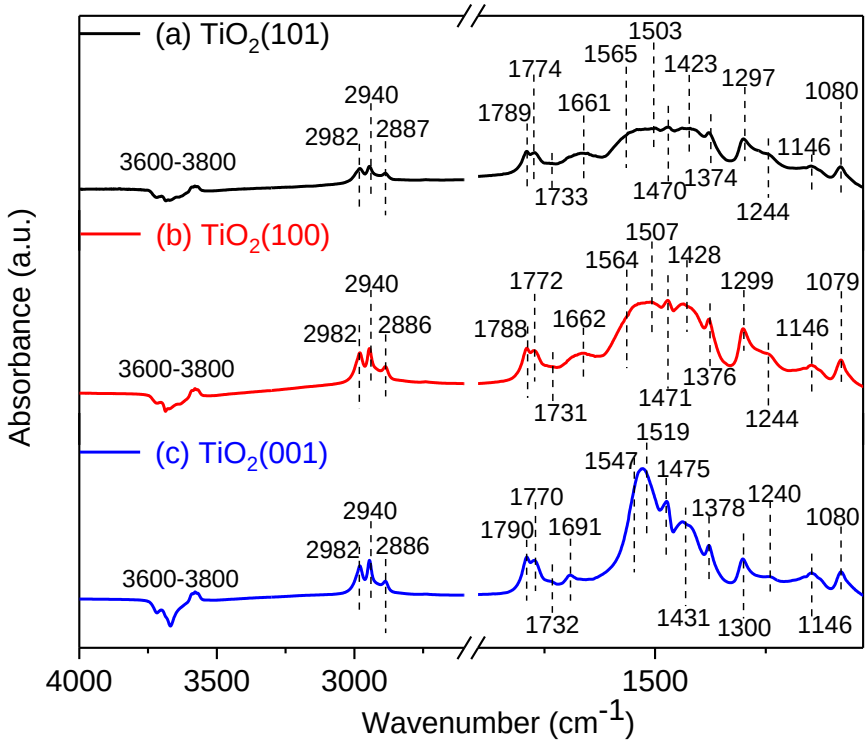

Fig. S14 IR spectra of propionic acid saturated adsorption on (a) TiO_2(101), (b) TiO_2(100) and (c) TiO_2(001) at 150 °C.

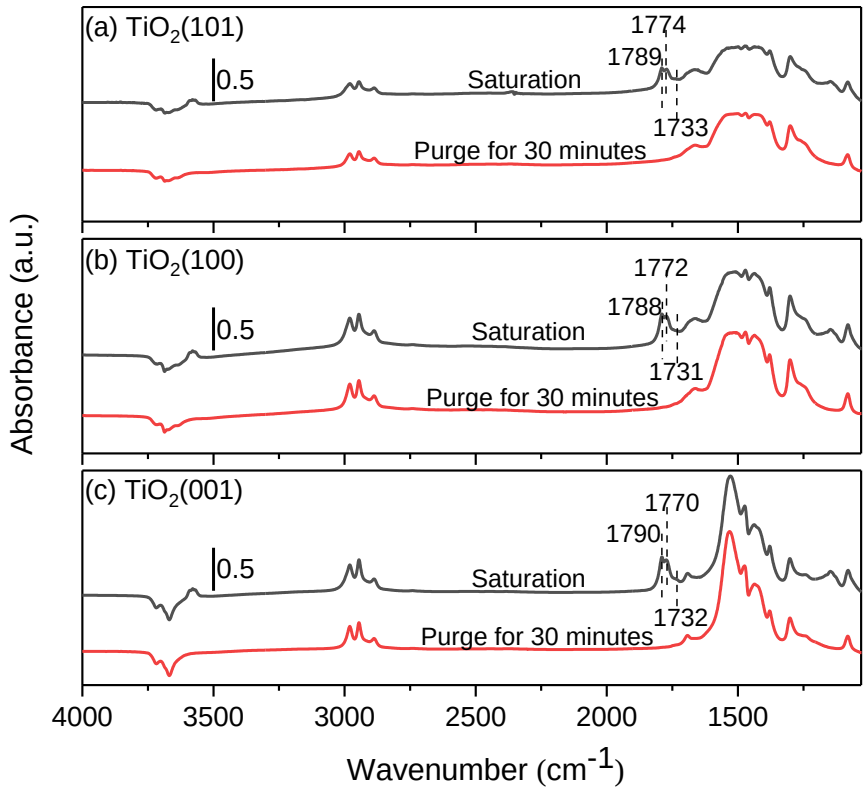

Fig. S15 IR spectra changes of (a) TiO_2(101), (b) TiO_2(100) and (c) TiO_2(001) with propionic acid saturated adsorption after purging in Ar flow at 150 °C.

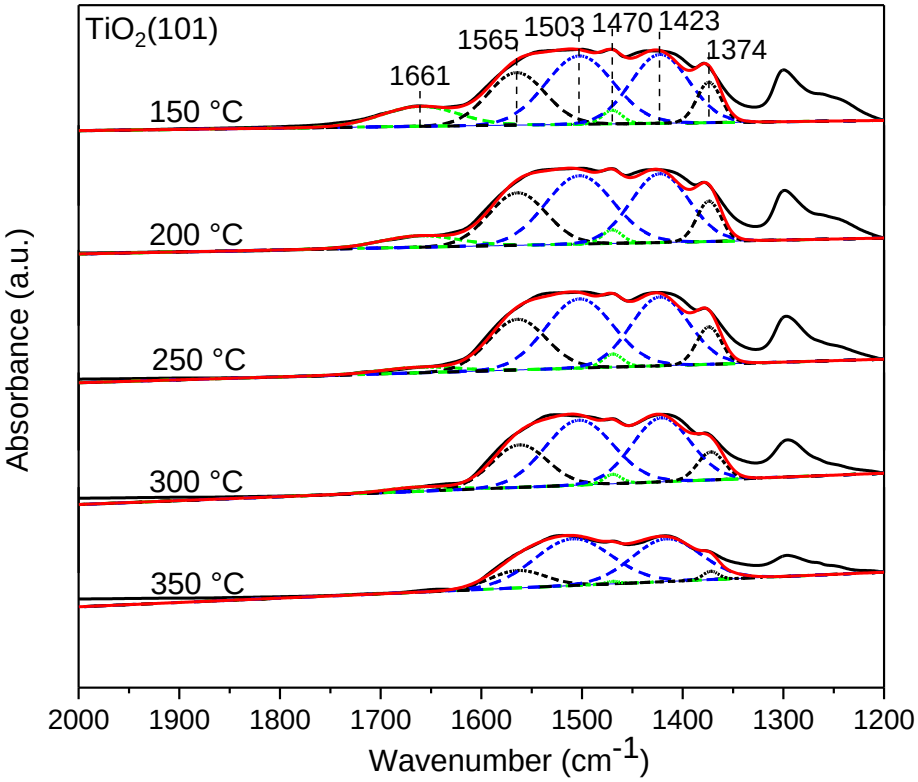

Fig. S16 In situ IR spectra on TiO_2(101) at 150 °C-350 °C.

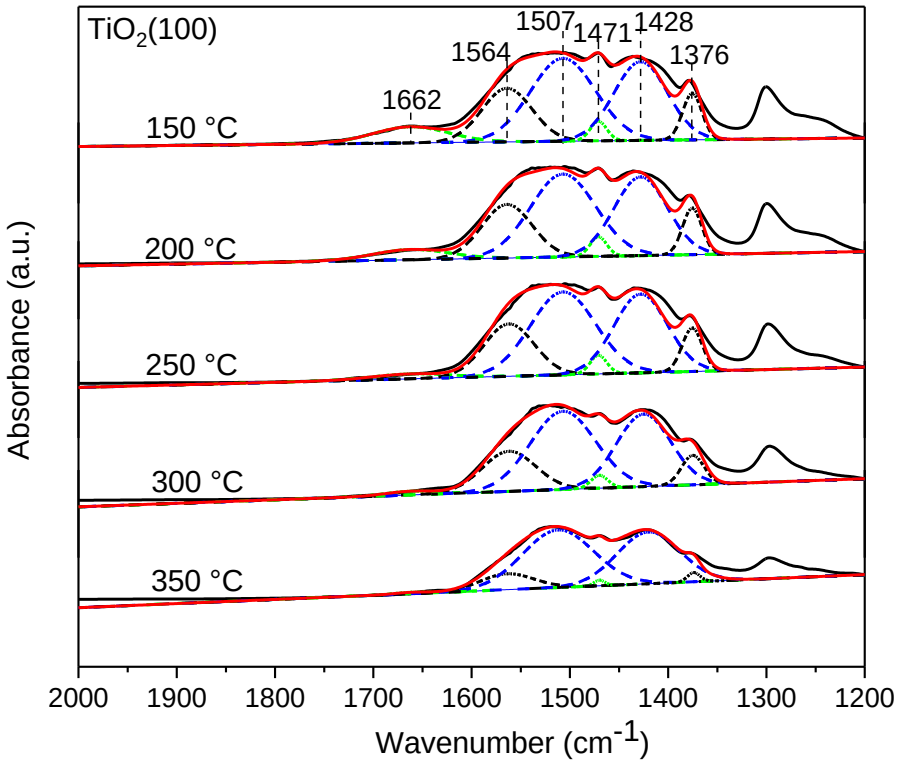

Fig. S17 In situ IR spectra on TiO_2(100) at 150 °C-350 °C.

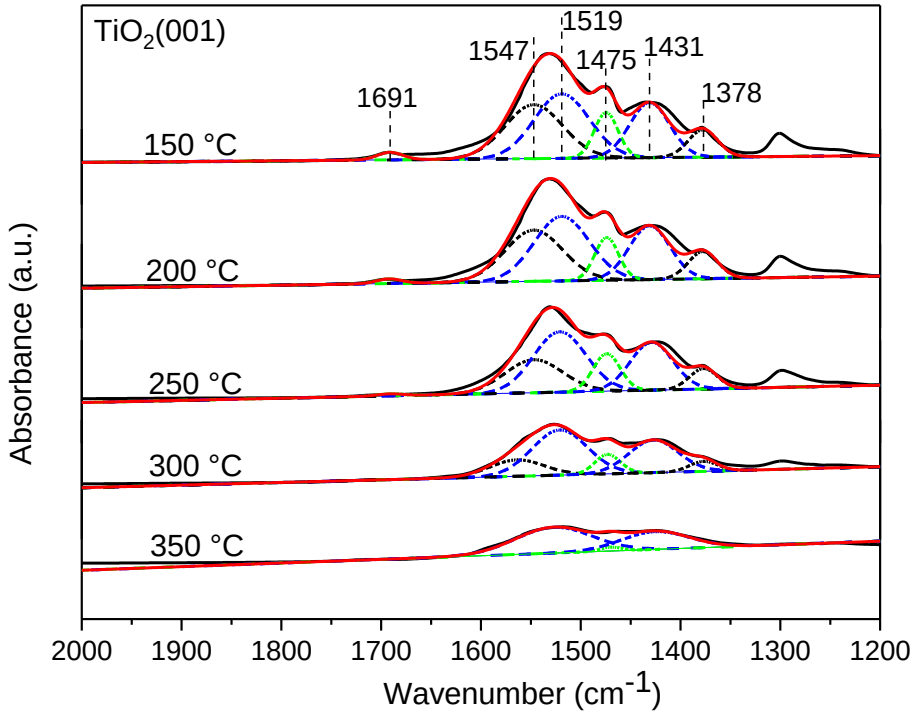

Fig. S18 In situ IR spectra on TiO_2(001) at 150 °C-350 °C.

Fig. S16-18 show curve fittings of IR spectra (the region of propionates) of TiO_2 catalysts during temperature programmed desorption of propionic acid. Solid lines represent experimental data and short dash lines represent the curve fitting data.

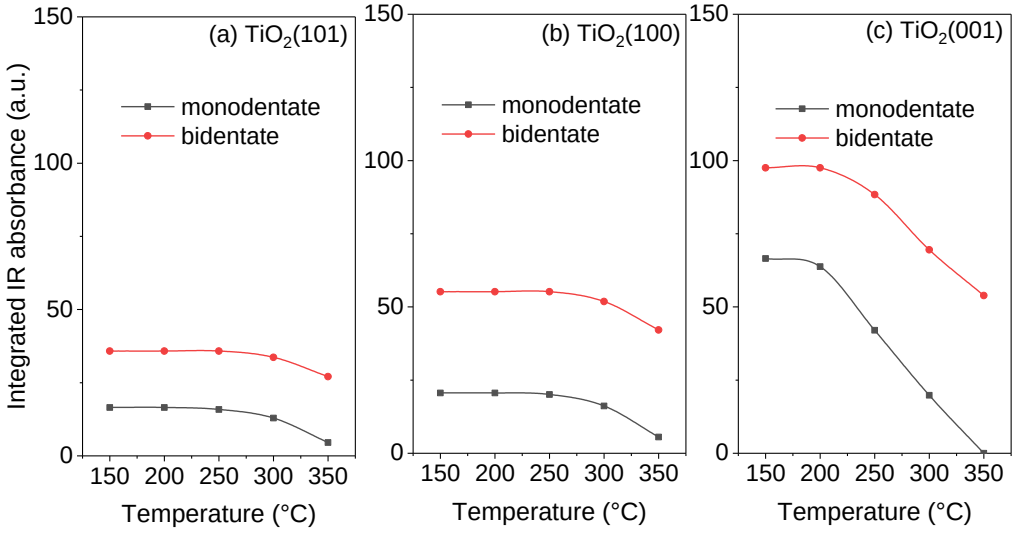

Fig. S19 Evolution of integrated bands areas of monodentate propionate and bidentate propionate based on surface area on (a) TiO_2(101), (b) TiO_2(100) and (c) TiO_2(001) as a function of temperature from 150 °C to 350 °C.

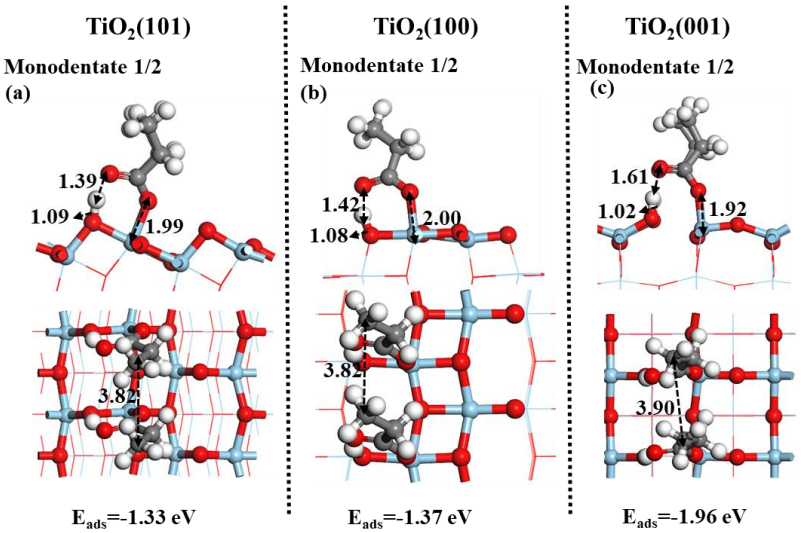

Fig. S20 DFT-determined monodentate propionate on TiO_2 (101), (100), and (001) surfaces at 1/2 ML (PBE + D3). The side and top views are shown in the top and bottom rows, respectively. Light blue, red, gray, and white spheres are Ti, O, C, and H atoms, respectively. The distances in the figure are given in Å. Ti and O atoms and Ti−O bonds in the lower layers are simplified as lines.

Table S2 DFT-surface energy of TiO_2 (101), (100), and (001) surfaces upon adsorption of propionic acid.

	Surface energy-monodentate (J/m^2)				Surface energy-bidentate (J/m^2)	
Acid coverage (ML)	0	1/4	1/2	1	1//4	1/2
TiO_2(101)	0.77	1.16	0.88	0.24	1.16	0.87
TiO_2(100)	0.87	1.43	1.10	0.46	1.33	0.94
TiO_2(001)	1.41	0.88	0.36	-0.21	0.87	0.33

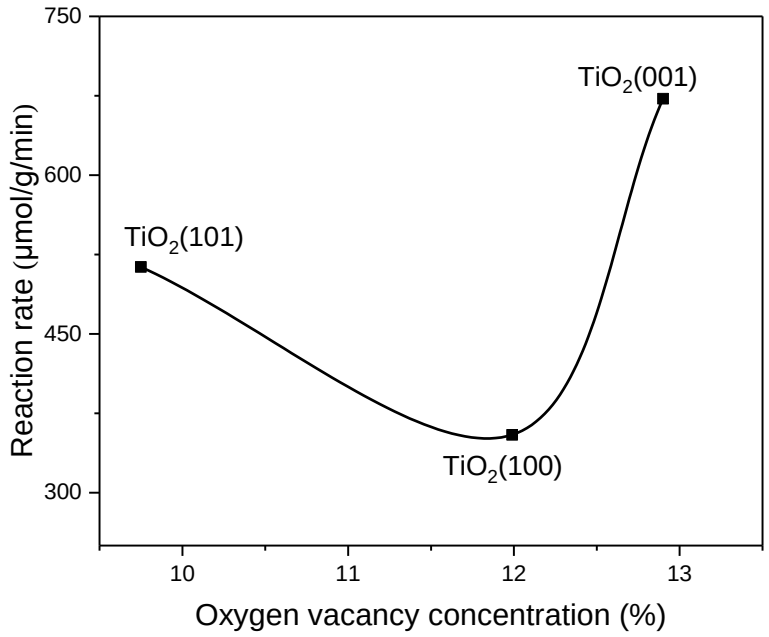

Fig. S21 Correlation between oxygen vacancy concentration and the intrinsic reaction rate.

Notes and references

1. E. V. Fufachev, B. M. Weckhuysen and P. C. A. Bruijnincx, *ChemSusChem*, 2021, **14**, 2710-2720.
2. M. Kobune, S. Sato and R. Takahashi, J. Mol. Catal. A: Chem., 2008, **279**, 10-19.
3. Y. Guo, Q. Yu, H. Fang, H. Wang, J. Han, Q. Ge and X. Zhu, *Ind. Eng. Chem. Res.*, 2020, **59**, 17269-17278.
4. Y. Guo, Y. Qin, H. Liu, H. Wang, J. Han, X. Zhu and Q. Ge, *ACS Catal.*, 2022, **12**, 2998-3012.
5. S. Ding, H. Wang, J. Han, X. Zhu and Q. Ge, Ind. Eng. Chem. Res., 2018, **57**, 17086-17096.
6. S. Ding, J. Zhao and Q. Yu, *Catalysts*, 2019, **9**, 768.
7. H. Ling, Z. Wang, L. Wang, C. Stampfl, D. Wang, J. Chen and J. Huang, *Catal. Today*, 2020, **351**, 58-67.
8. J. A. Bennett, C. M. A. Parlett, M. A. Isaacs, L. J. Durndell, L. Olivi, A. F. Lee and K. Wilson, *ChemCatChem*, 2017, **9**, 1648-1654.
9. J. A. Lopez-Ruiz, A. R. Cooper, G. Li and K. O. Albrecht, *ACS Catal.*, 2017, **7**, 6400-6412.
10. F. Lu, B. Jiang, J. Wang, Z. Huang, Z. Liao and Y. Yang, *Mol. Catal.*, 2018, **444**, 22-33.
11. H. Bayahia, E. F. Kozhevnikova and I. V. Kozhevnikov, *Appl. Catal., B*, 2015, **165**, 253-259.